Allosteric Regulation of *Bacillus subtilis* Threonine Deaminase, a Biosynthetic Threonine Deaminase with a Single Regulatory Domain[†]

Anat Shulman,[‡] Elena Zalyapin,[‡,§] Maria Vyazmensky,[‡] Ofer Yifrach,[‡,||] Ze'ev Barak,[‡] and David M. Chipman*[,‡]

Department of Life Sciences, Ben-Gurion University of the Negev, P.O. Box 653, Beer Sheva 84105, Israel, and Zlotowski Center for Neuroscience, Ben-Gurion University of the Negev, P.O. Box 653, Beer Sheva 84105, Israel

Received May 14, 2008; Revised Manuscript Received August 19, 2008

ABSTRACT: The enzyme threonine deaminase (TD) is a key regulatory enzyme in the pathway for the biosynthesis of isoleucine. TD is inhibited by its end product, isoleucine, and this effect is countered by valine, the product of a competing biosynthetic pathway. Sequence and structure analyses have revealed that the protomers of many TDs have C-terminal regulatory domains, composed of two ACT-like subdomains, which bind isoleucine and valine, while others have regulatory domains of approximately half the length, composed of only a single ACT-like domain. The regulatory responses of TDs from both long and short sequence varieties appear to have many similarities, but there are significant differences. We describe here the allosteric properties of *Bacillus subtilis* TD (*bsTD*), which belongs to the short variety of TD sequences. We also examine the effects of several mutations in the regulatory domain on the kinetics of the enzyme and its response to effectors. The behavior of *bsTD* can be analyzed and rationalized using a modified Monod−Wyman−Changeux model. This analysis suggests that isoleucine is a negative effector, and valine is a very weak positive effector, but that at high concentrations valine inhibits activity by competing with threonine for binding to the active site. The behavior of *bsTD* is contrasted with the allosteric behavior reported for TDs from *Escherichia coli* and *Arabidopsis thaliana*, TDs with two subdomains. We suggest a possible evolutionary pathway to the more complex regulatory effects of valine on the activity of TDs of the long sequence variety, e.g., *E. coli* TD.

Metabolic control of biosynthetic pathways is often achieved by allosteric regulation of key enzymes along the pathway (*1*). In many instances, the first committed step along such a pathway is catalyzed by an allosteric enzyme that is subject to feedback inhibition by the end product of the pathway, thus downmodulating the biosynthesis of the product (*2, 3*). Threonine deaminase (TD),[1] a pyridoxal phosphate-dependent enzyme which catalyzes the first committed step in the isoleucine biosynthetic pathway (*4, 5*) (Figure 1), was one of the earliest such enzymes to be studied (*6*). TD converts threonine to 2-ketobutyrate which is the precursor for further enzyme-catalyzed reactions. In many organisms, TD has been shown to be inhibited by isoleucine, the end product of the pathway, and activated by valine, the end product of the parallel competing pathway (Figure 1) (*6*−*14*). Detailed studies on TD from several species (*8, 12, 14, 15*), particularly *Escherichia coli* (*13, 16*−*19*), demonstrated that TD is an allosteric enzyme exhibiting homotropic cooperativity with respect to threonine and heterotropic interactions with respect to valine and isoleucine, which are the allosteric activator and inhibitor, respectively.

The three-dimensional structure of TD from *E. coli* (*ecTD*) (*20*) has stimulated attempts to rationalize the allosteric properties of the enzyme. The *ecTD* enzyme is a homotetramer whose subunits are each composed of a catalytic domain and a regulatory domain (Figure 2A). The regulatory domain is in turn composed of two tandem ACT-like subdomains (*21*) (Figure 2B) related by a pseudosymmetric two-fold axis (*4, 14, 20*). The two ACT-like subdomains of a single polypeptide interact to form a fold similar to that of the regulatory domains observed in 3-phosphoglycerate dehydrogenase (3-PGDH) (Figure 2C) (*4, 20, 22*). On the basis of the structural similarity with the 3-PGDH regulatory domain and mutational analysis, the putative valine and isoleucine effector binding sites of *ecTD* and *Arabidopsis thaliana* TD (*atTD*) have been mapped to a region at the interface between the two ACT-like subdomains (*4, 14, 20*). Wessel and co-workers (*14*) have pointed out that the two regulatory binding sites in such a tandem pair of ACT-like subdomains can be intrinsically different. However, the TD sequences from many other species lack the second C-terminal ACT-like subdomain (*20, 21*) (Figure 2D; see also Figure 1 of the Supporting Information). In this study, we have investigated the allosteric properties of threonine deaminase from *Bacillus subtilis* (*bsTD*), which has only a

[†] This research was supported by the Israel Science Foundation (Grants 467/02 to Z.B. and 716/06 to Boaz Shaanan and D.M.C.).

* To whom correspondence should be addressed. E-mail: chipman@bgu.ac.il. Phone: ++972-8-647 2646. Fax: ++972-8-647 9173.

[‡] Department of Life Sciences.

[§] Present address: Center for Systems Biology, Richard B. Simches Research Center, Massachusetts General Hospital, 185 Cambridge St., Boston, MA 02114.

[||] Zlotowski Center for Neuroscience.

[1] Abbreviations: TD, threonine deaminase; *bsTD*, threonine deaminase from *B. subtilis*; *ecTD*, threonine deaminase from *E. coli*; *atTD*, threonine deaminase from *A. thaliana*; PLP, pyridoxal phosphate; AB, aminobutyrate; TAPS, *N*-tris(hydroxymethyl)methyl-3-aminopropanesulfonic acid; DNPH, 2,4-dinitrophenylhydrazine; PMSF, phenylmethanesulfonyl fluoride; MALDI-TOF, matrix-assisted laser desorption ionization time-of-flight mass spectrometry.

10.1021/bi800901n CCC: $40.75
Published on Web 10/15/2008

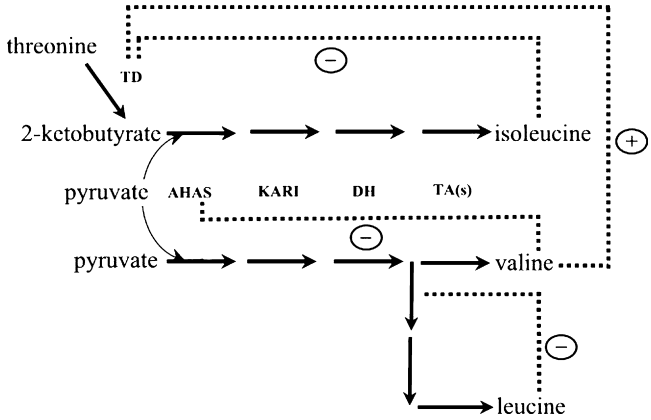

FIGURE 1: Metabolic network of branched chain amino acids synthesis. The flux through the competing biosynthetic pathways of the branched chain amino acids leucine, isoleucine, and valine is tightly controlled by allosteric regulation of key enzymes along the pathways. Threonine deaminase (TD) is the first committed enzyme for the biosynthesis of isoleucine. Acetohydroxyacid synthase (AHAS) is the first of four enzymes common to both the isoleucine and valine pathways. This enzyme catalyzes the first committed step in the biosynthesis of valine and leucine by decarboxylation of pyruvate and condensation of the resulting two-carbon moiety with a second molecule of pyruvate, or the second step in the competing isoleucine pathway by condensation of the pyruvate-derived two-carbon moiety with 2-ketobutyrate. The other three enzymes common to both these pathways are ketol-acid reductoisomerase (KARI), dihydroxyacid dehydratase (DH), and transaminase (TA), which catalyze the formation of precursors leading to isoleucine and valine. End product regulation of the different enzymes along the network is shown by the dotted lines with the + and − signs representing allosteric activation and inhibition effects, respectively.

single ACT-like domain. This structural difference raises an interesting question: How is it that the regulatory function of *bsTD* is qualitatively similar to those of *ecTD* and *atTD*, even though the former lacks the second ACT-like subdomain which forms the complete regulatory domain in the latter proteins?

In this study, we analyze the allosteric behavior of *bsTD*. Our results are consistent with a Monod−Wyman−Changeux scheme for regulation of *bsTD* by valine and isoleucine that is different from that proposed for *ecTD* (*4, 13, 16*−*18, 20, 23*) and *atTD* (*14, 24*). We propose a model for the regulatory domain organization of *bsTD* (Figure 2D) and investigate the allosteric properties of several variants of *bsTD* with mutations in the region of the putative effector binding sites. The kinetic behavior of the *bsTD* variants is consistent with both the kinetic scheme and the proposed structural model. A possible evolutionary relationship between *bsTD* and those threonine deaminases with two ACT-like regulatory subdomains is discussed.

EXPERIMENTAL PROCEDURES

L-Threonine was obtained from Duchefa Biochemie BV (Haarlem, The Netherlands). Pyridoxal-5-phosphate monohydrate (PLP) was purchased from Fluka (Darmstadt, Germany). L-Isoleucine, L-valine, 2-ketobutyrate, *N*-tris(hydroxymethyl)methyl-3-aminopropanesulfonic acid (TAPS), and 2,4-dinitrophenylhydrazine (DNPH) were from Sigma-Aldrich (St. Louis, MO). Hydroxylapatite was purchased from Bio-Rad Laboratories (Hercules, CA), and Toyopearl Butyl-650S was from TosoHaas.

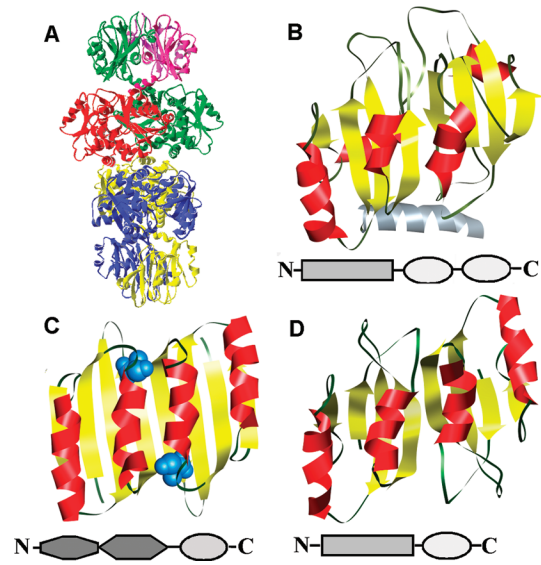

FIGURE 2: (A) Schematic representation of the structure of threonine deaminase from *E. coli* (*ecTD*), based on PDB entry 1TDJ (*20*), in a ribbon representation. The regulatory domains are at top and bottom of the picture in this view and the catalytic domains in the center. Each chain in the homotetramer is shown in a different color, with the catalytic domain of one of the four chains colored red and its regulatory domain colored with pink to purple shades. (B−D) Schematic ribbon diagrams of regulatory domains of different enzymes with α-helices colored red and *β*-strands yellow. A schematic sequence domain sketch of the complete polypeptide is shown under each structure (see Figure 1 of the Supporting Information). Dark gray rectangles or polygons represent the enzymes' catalytic domains, and white ovals represent the C-terminal regulatory ACT-like subdomains. Panel B is the regulatory domain of threonine deaminase from *E. coli* (*ecTD*) (as shown in pink in part A), seen from a different angle. The gray helix is a link between the C-terminus of the catalytic domain, and the beginning of the regulatory domain. Panel C is a dimer of regulatory domains of 3-phosphoglycerate dehydrogenase (3-PGDH) from *E. coli* (based on PDB entry 1PSD). Panel D is our tentative model for a dimer of regulatory domains of *bsTD*. The model for the monomer was prepared using the PHYRE server (http://www.sbg.bio.ic.ac.uk/phyre/html/index.html) (*38*) based on the homology of the regulatory domain of *bsTD* with the first regulatory subdomain of *ecTD*. The dimer was then modeled assuming it has the symmetry of paradigmatic dimeric ACT domain of 3-PGDH and the pseudosymmetry of the *ecTD* regulatory domain (*20*).

Protein Expression and Purification. The *ilvA* gene of *B. subtilis* encoding TD was cloned into a modified pQE vector (*25*) between *Nde*I and *Hin*dIII unique restriction sites, to produce vector pQEVA. Mutations were introduced into pQEVA by the PCR overlap extension method (*26*). The resulting mutated sequences were verified.

The vectors were transformed into *E. coli* XL-1 MRF (Stratagene Europe, Amsterdam, The Netherlands) cells. Transformed cells were grown in TB medium at 37 °C to a turbidity of 1 OD_{600}, induced (0.5 mM IPTG), and grown overnight at 20 °C. Cells were harvested by centrifugation. The pellet was resuspended in a buffer at pH 7.5 containing 50 mM potassium phosphate, 1 mM dithiothreitol, 1 mM EDTA, 1 mM isoleucine (or 10 mM isoleucine in the case of mutants L352A and Y371L), 1 mM pyridoxal phosphate, and 0.15 mM PMSF, sonicated, and centrifuged at 28000*g* for 1 h at 20 °C. The fractions containing the target protein were then precipitated using 22% (w/v) ammonium sulfate. Following resuspension, the protein was loaded onto a hydroxylapatite column and the flow-through was collected.

This treatment does not lead to any significant increase in protein purity but is necessary to confer cold resistance to the enzyme (*27*). The hydroxylapatite flow-through was loaded onto a reversed-phase Toyopearl Butyl-650S column, and bound protein was eluted by applying a gradient of decreasing ammonium sulfate concentrations (0.8 to 0 M). The most active fractions were collected. The protein purity was >95% as judged by SDS−PAGE.

The purified protein was stripped of bound isoleucine by dialysis or by the Penefsky centrifuged column method (*28*) and used at once or stored at 4 °C. We found that the purified protein slowly lost activity even under these conditions, and all quantitative kinetic experiments reported here were carried out with protein samples stored for less than 1 month. The mutant L352A was unstable in the absence of isoleucine and was therefore stored with 10 mM isoleucine.

Wild-type *bsTD* proteins are homotetramers. The molecular mass of the protomer was calculated from the plasmid sequence to be 47 kDa. This was confirmed by SDS−PAGE calibrated with appropriate standards, as well as by MALDI-TOF showing the 47 kDa monomer peak and a peak corresponding to a tetramer, with a molecular mass of 188 kDa (data not shown). The holoenzyme size was further confirmed by migration distances in native gradient PAGE and dynamic light scattering. FPLC of the purified protein on a Superdex 75 size exclusion column showed a single sharp peak at an elution volume corresponding to a molecular mass of 190 kDa (Y. Zherdev, personal communication).

Steady-State Rates of Threonine Deamination. TD-catalyzed formation of 2-ketobutyrate was assessed colorimetrically (*15*) at 37 °C in 0.4 M TAPS buffer (pH 7.8) containing different concentrations of threonine, with or without addition of isoleucine and/or valine. The reaction was initiated by addition of the enzyme and stopped by adding 3.5 mL of DNPH dissolved in 0.5 M HCl. The formation of 2-ketobutyrate in this assay was linear for at least 20 minutes, and we chose to stop the reaction at 15 min in the standard assay. The formation of the colored ketobutyrate−DNPH complex was stopped after an additional 15 min by adding 1 mL of 40% KOH, and the product absorption was measured at 600 nm. The sodium salt of 2-ketobutyrate was used for the calibration curve.

Fluorescence Measurements of Binding of the Substrate Analogue Aminobutyrate (AB) to bsTD. Fluorescence experiments were performed using a Perkin-Elmer fluorimeter at an excitation wavelength of 400 nm and an emission wavelength of 485 nm. Experiments were performed at 37 °C with enzyme monomer concentrations of 0.7−2.1 μM. An average of three emission spectra was used to compute the relative fluorescence. ΔF was calculated by subtracting the basal pyridoxal phosphate cofactor (PLP) fluorescence of the enzyme from the stimulated PLP fluorescence after addition of AB. F_{max} is the maximal fluorescence change induced by substrate analogue binding and is estimated from the saturation curve using Hill analysis (*29*), while $\Delta F/F_{max}$ is assumed to be directly proportional to the fractional binding saturation. The variance in the fluorescence changes upon AB binding to *bsTD* at each substrate concentration did not exceed 6%.

Data Analysis. Steady-state kinetics of threonine deamination or substrate analogue binding to *bsTD* were fitted to the phenomenological Hill equation (*29*) using SigmaPlot (version 6, Jandel Corp.):

$$V = (V_{max}[S]^{n_H})/(K^{n_H} + [S]^{n_H}) \quad (1)$$

Analysis of steady-state binding or catalysis data according to a Monod−Wyman−Changeux (MWC) symmetrical model was performed by fitting the experimental data in the presence of different threonine concentrations and in the presence and absence of different concentrations of valine and isoleucine to an equation derived from a modified MWC model. The initial model took into account two assumptions: (a) Threonine binds to the active sites of *bsTD* with a preference for the R state, and the enzymatic reaction takes place only in the R state; (b) the allosteric effectors isoleucine and valine bind to the regulatory sites of the enzyme. The binding of valine in a given effector site excludes simultaneous isoleucine binding in the same site, and vice versa. Each effector has a characteristic affinity and preference for the two states of the enzyme.

These assumptions lead to eq 2 (*30*):

$$\bar{Y} = V/V_{max} = \alpha(1+\alpha)^3/[(1+\alpha)^4 + LA^4(1+c_S\alpha)^4] \quad (2)$$

where $\bar{Y}$ is the fractional binding saturation proportional to V/V_{max}, L (=[T]/[R]) is the allosteric equilibrium constant of *bsTD* in the absence of any ligands, α (=[Thr]/K_R) is the ratio of the threonine concentration to the dissociation constant of threonine from the R state, and c_s ($=K_R^S/K_T^S$) is the ratio of dissociation constants of the substrate, threonine, from the R and T conformations. A in eq 2 represents the combined effects of the amino acid modulators bound in the regulatory sites on the allosteric equilibrium and is defined in eq 3:

$$A = (1 + c_I\gamma + c_V\delta)/(1 + \gamma + \delta) \quad (3)$$

where $\gamma = [Ile]/K_R^{Ile}$ and $\delta = [Val]/K_R^{Val}$ and are the ratios of isoleucine and valine concentrations to the dissociation constants of these amino acids from the effector sites in the R conformation, respectively, and c_I and c_V are the ratios of the dissociation constants of the two effector amino acids from the regulatory sites in the R and T conformations.

The experimental results required us to consider the existence of an additional interaction of valine with the enzyme: binding to the active sites, in competition with substrate. Equation 4 includes this interaction:

$$\bar{Y} = V/V_{max} = \alpha(1+\alpha)^3/[(1+\alpha+\beta)^4 + LA^4(1+c_S\alpha+c_{Vin}\beta)^4] \quad (4)$$

where β [=[Val]/$K_{R(act)}^{Val}$] is the ratio of the valine concentration to the dissociation constant of valine from the active (catalytic) site in the R state and c_{Vin} [$=K_{R(act)}^{Val}/K_{T(act)}^{Val}$] is the ratio of the dissociation constants of valine from the catalytic sites in the R and T conformations. The results of kinetic experiments justify this additional assumption, as do the behaviors of regulatory mutants of *bsTD*.

We were able to fit all the steady-state data for a given protein variant with a consistent set of parameters in two steps, first a simultaneous fit of all data in the absence of valine and then fit of the remaining data while assuming the parameters unrelated to valine were known. The reliability of this procedure was then tested by circular repetition of the fit to all data, each time with only one or two parameters

assumed known from previous fits. In some cases, the data for a variant could be fit only by assuming an approximate value for a poorly determined parameter such as $K^{Val}_{R(act)}$ or c_{Vin} (see Results).

Throughout this paper, we report estimates of parameters ± standard errors as given by SigmaPlot, which are 95% confidence intervals for the true values of the parameters. R^2 values for all fits in this study were greater than 0.985. The *P* values for the calculated parameters were <0.0001, unless otherwise stated.

RESULTS

The major goal of this study was to analyze the allosteric regulation of *B. subtilis* TD and explain its behavior on the basis of a structural model for the enzyme. We hoped to be able to understand the relationship between the functional properties of *bsTD* and *ecTD*, two enzymes with different regulatory domain architectures. We began with the examination of the allosteric properties of *bsTD*, partially characterized in the early 1970s (*15*). The detailed analyses by Eisenstein and colleagues of the allosteric properties of TD from *E. coli* inspired the re-examination of *bsTD* using contemporary methods (*16, 18, 23*). We then used the tentative identification of the ligand-binding sites in *ecTD* and *atTD* (*14, 17, 19, 24*) and multiple alignments to ACT domains in other proteins (*21*) to identify residues which might be involved in the binding of the allosteric effectors. We tested these assignments by site-directed mutagenesis and analysis of the kinetic properties of the mutants.

Positive Cooperativity in bsTD. Initial rates of threonine deamination by *B. subtilis* TD were measured as a function of threonine concentration. The threonine dependence of the steady-state rate is sigmoidal (Figure 3A), and a fit of the data to the Hill equation (*29*) yields a $K_{0.5}$ of 9.6 ± 0.7 mM and a value of 1.27 ± 0.10 for the Hill coefficient (Table 1), a low value considering the tetrameric organization of *bsTD*. It is important to note here that if care is not taken to strip isoleucine from *bsTD* samples, the shift in the conformational equilibrium caused by isoleucine binding would raise the apparent Hill coefficient for substrate. However, the enzyme preparations we used here were subjected to several steps which should have removed any exchangeable isoleucine (see Protein Expression and Purification in Experimental Procedures). In any case, this low level of cooperativity would have been difficult for previous investigators to observe from their data (*15*).

The binding of aminobutyrate (AB) to the active site of TD was also examined. AB is a substrate analogue that cannot be turned over by TD (*23*) but upon binding induces changes in PLP fluorescence similar to those seen with threonine. AB binding to *bsTD* (Figure 3B) is also sigmoidal with a Hill coefficient value of 1.31 ± 0.03 and a K_d of 52.3 ± 2.9 mM. The sigmoidal profiles obtained in both steady-state catalysis and binding experiments demonstrate the existence of positive cooperativity in ligand binding to the active site of *bsTD*, as seen with TD from other species (*8, 18, 31*).

Allosteric Regulation of bsTD by Isoleucine. Initial rates of threonine deamination by *bsTD* were measured as a function of isoleucine concentration in the presence of 10, 20, and 50 mM threonine (Figure 4A) and the results fit to the Hill equation (Table 2). Three aspects of the results should be noted. (1) The effect of isoleucine on *bsTD* activity shows a cooperative dependence on the concentration of the effector (note that this and several other graphs in this paper

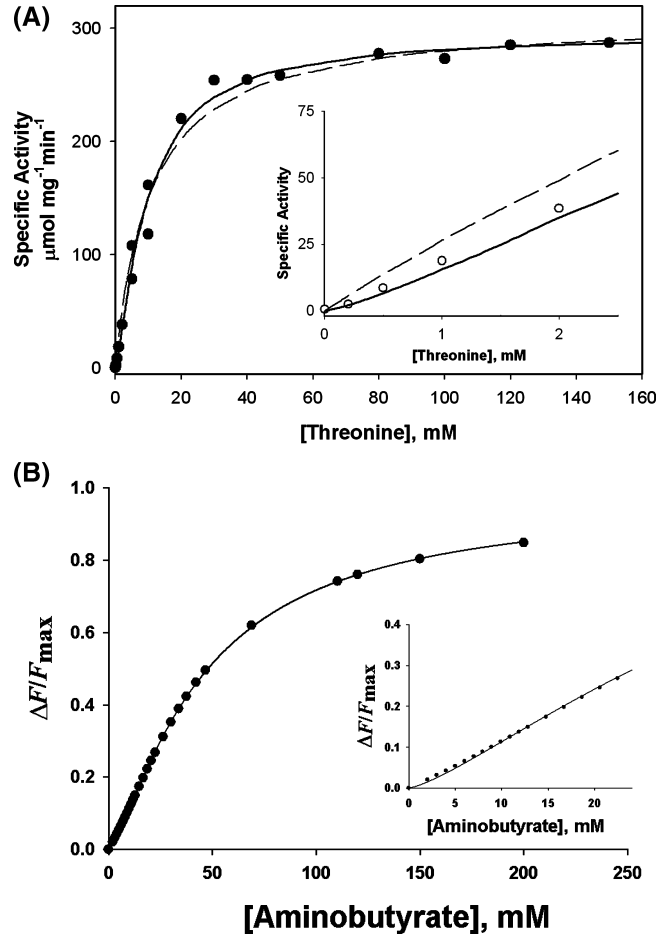

FIGURE 3: Positive cooperativity of *bsTD* in the absence of effectors. In each case, the oligomer concentration of *bsTD* was ~2.7 nM and the reactions were carried out at 37 °C as described in Experimental Procedures. The data were fitted to the Hill equation (*29*). (A) Dependence of the initial velocity of threonine deamination by *bsTD* on the threonine concentration in the absence of any effectors. The insert magnifies the low substrate region. The apparent $K_{0.5}$ for threonine determined from the catalytic activity is 9.6 ± 0.66 mM with a Hill coefficient (n_H) of 1.27 ± 0.11. For comparison, the fit of the data to the Michaelis−Menten equation is shown as a dashed line. (B) Change in the fluorescence of the active site PLP induced by aminobutyrate binding to *bsTD*. The inset in panel B magnifies the observed changes at low concentrations of AB. The apparent $K_{0.5}$ for AB binding in the active site is 52.3 ± 2.9 mM, with a Hill coefficient (n_H) of 1.31 ± 0.03.

Table 1: Hill Analysis (*29*) of the Effects of Valine and Isoleucine on the Cooperativity in Threonine Binding and Catalysis by *bsTD*[a]

	steady-state kinetics		AB binding	
	$K_{0.5}$ (mM)	n_H	$K_{0.5}$ (mM)	n_H
no effectors	9.6 ± 0.7	1.27 ± 0.10	52.3 ± 2.9	1.31 ± 0.03
with 0.1 mM Ile	ND[b]	ND[b]	106 ± 10	1.64 ± 0.6
with 0.3 mM Ile	26.6 ± 0.6	1.88 ± 0.07	ND[b]	ND[b]
with 30 mM Val	12.8 ± 0.9	1.19 ± 0.09	ND[b]	ND[b]
with 0.3 mM Ile and 30 mM Val	14.4 ± 0.7	1.37 ± 0.09	ND[b]	ND[b]

[a] Steady-state threonine deaminase catalysis and aminobutyrate binding data for *bsTD* were fitted to the Hill equation (*29*). The values of $K_{0.5}$, the apparent dissociation constant for the substrate, and of n_H for the substrate obtained under different conditions are indicated for both analyses. [b] Values not determined under these conditions.

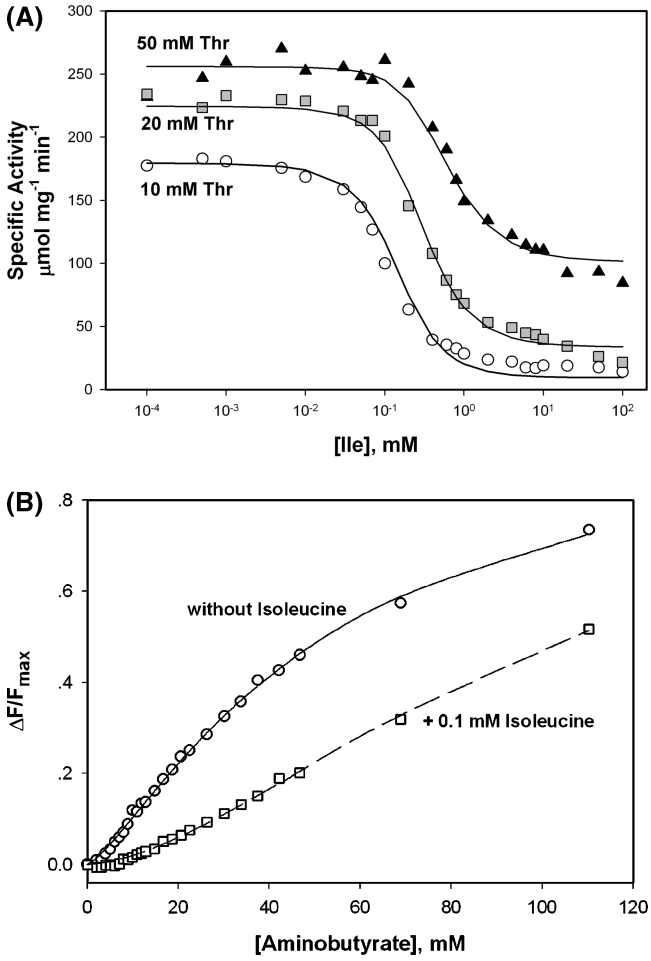

FIGURE 4: Influence of isoleucine on *bsTD*. (A) Initial velocity of threonine deamination by *bsTD* as a function of isoleucine concentration in the presence of 10 (○), 20 (■), or 50 mM threonine (▲). Data were fit to eq 2 as described in the text. (B) Change in the fluorescence of the active site PLP induced by aminobutyrate binding to *bsTD* in the presence (□) or absence (○) of 0.1 mM isoleucine. The data were fit to the Hill equation (parameters in Table 1).

Table 2: Hill Analysis of Isoleucine Inhibition of Wild-Type *bsTD*[a]

	10 mM threonine	20 mM threonine	50 mM threonine
$K_{0.5(Ile)}$ (mM)	0.110 ± 0.004	0.282 ± 0.019	0.740 ± 0.088
n_H	1.42 ± 0.07	1.33 ± 0.10	1.40 ± 0.24
V (μmol mg^{-1} min^{-1})	179 ± 2	232 ± 3	255 ± 4
ΔV (μmol mg^{-1} min^{-1})	160 ± 2	196 ± 4	156 ± 7

[a] Steady-state catalysis data for *bsTD* at three substrate concentrations (Figure 4A) were fit to the Hill equation (*29*), and values for $K_{0.5(Ile)}$ (the apparent inhibition constant for isoleucine), n_H, V (maximum velocity), and ΔV (extrapolated decrease in velocity at saturation with isoleucine) are given.

have logarithmic scales), with an $n_{H(Ile)}$ of 1.3−1.4. (2) $K_{0.5(Ile)}$ increases with an increase in substrate concentration. (3) The inhibitory effect of isoleucine on *bsTD* activity levels off at 10−30% residual activity. The binding of the substrate analogue AB to *bsTD* is also affected by the presence of isoleucine (Figure 4B), as expected. K_d for aminobutyrate is increased by ~2-fold in the presence of 0.1 mM isoleucine, and the apparent cooperativity of binding increases as expected (Table 1). Other biosynthetic TDs exhibit similar effects of isoleucine (*8, 12*−*14, 23, 31*).

Table 3: A Modified MWC Model for *bsTD* Accounts for Steady-State Catalysis, AB Binding, and the Effects of Isoleucine on Both

parameter[a]	steady-state catalysis	AB binding
L	2.61 ± 0.13	2.4 ± 0.3
K_R^S (mM)	6.02 ± 0.36	38 ± 3
c_S	0.149 ± 0.012	0.20 ± 0.02
K_R^{Ile} (mM)	0.379 ± 0.028	0.27 ± 0.02[b]
c_I	3.50 ± 0.19	3.5 ± 0.1[b]

[a] Values for parameters obtained by fitting of the steady-state threonine deamination data (Figures 3A and 4A) or equilibrium aminobutyrate binding data (from fluorescence) for *bsTD* (Figures 3B and 4B) to eq 1. Correlation coefficients of >0.995 were obtained for *bsTD* catalysis and binding data. Parameter definitions are given in Data Analysis. [b] The correlation coefficient for K_R^{Ile} and c_I in the analysis of AB binding data was near unity, so that these two parameters could be determined only separately.

Analysis of the data of each of these experiments with the MWC model (eq 2, or the equivalent eq 4 with [Val] = 0) gave a good fit and allowed us to determine K_R^S, c_S, K_R^{Ile}, c_I with $P < 0.0001$, and L with $P = 0.0002$. The results are listed in Table 3.

Allosteric Regulation of bsTD by Valine. When care was taken to remove isoleucine from the purified wild-type *bsTD*, valine did not cause statistically significant activation of the enzyme but did lead to a decrease in substrate cooperativity (Table 1). High concentrations of valine (≥10 mM) led to inhibition (Figure 5A), in agreement with the first reports on the regulation of *bsTD* (*15*).

However, in the presence of 0.1−1 mM isoleucine, valine led to a complex biphasic effect on *bsTD* (Figure 5B). At a given isoleucine concentration, an increasing valine concentration first relieves the inhibition caused by isoleucine but, with a further increase, inhibits. This behavior is different from that observed for other TD species (*8, 14, 17*), for which valine was found to be an activating ligand only. The biphasic effect of valine on the activity of *bsTD* suggests that valine binds at two distinct sites on the enzyme. The activating effect of valine is observed in wild-type *bsTD* only under conditions where a significant fraction of the enzyme would otherwise be in the T state, e.g., in the presence of inhibiting concentrations of isoleucine (see Figure 5B). The MWC model of eq 4 rationalizes this effect in terms of competition between valine and isoleucine at the same regulatory sites. The examination of the behavior of mutant forms of *bsTD* supports this hypothesis. On the other hand, the inhibitory effect of valine can best be explained as arising from competition with threonine at the active sites.

The complex response of the enzyme activity to valine in the presence of isoleucine can be fit to the expanded MWC equation we suggest above (eq 4), with nine parameters. We assumed the values of L, K_R^S, c_s, K_R^{Ile}, and c_I found from the substrate dependence and isoleucine inhibition of threonine deamination (Figures 3A and 4A) and derived the values of the three remaining parameters ($K_{R(act)}^{Val}$, K_R^{Val}, and c_{Vin}) with good statistical significance with a simultaneous fit of all the data of Figure 5A,B (Table 4). The binding of valine to the regulatory sites shows little dependence on the allosteric state of the enzyme; that is, c_V (K_R^{Val}/K_T^{Val}) is not statistically different from 1.

Effector Binding Sites in the bsTD Regulatory Domain. A tentative model for the regulatory domain of *bsTD* was constructed using the experimental structure of *ecTD* (*20*)

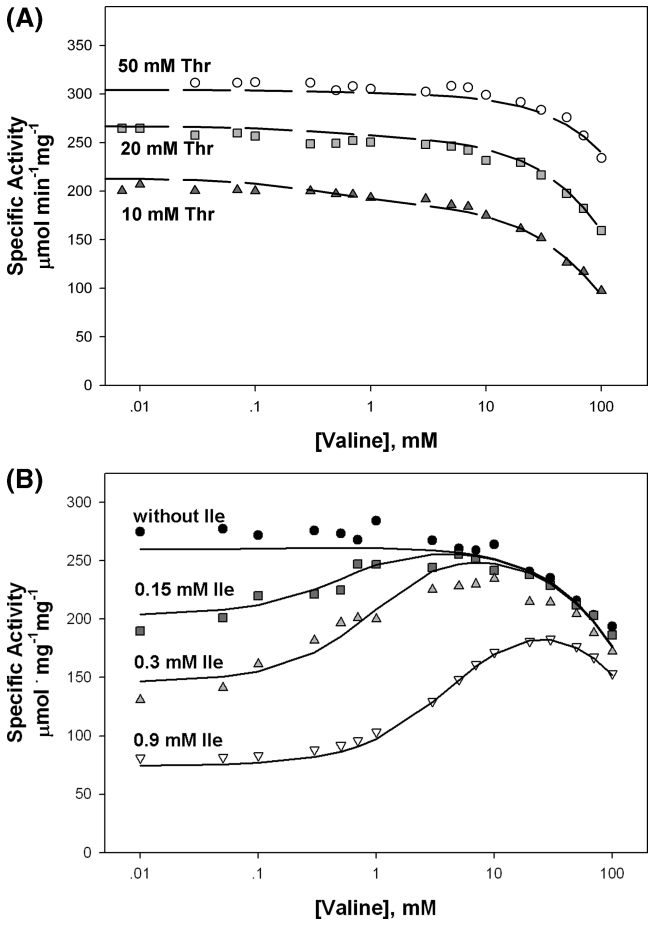

FIGURE 5: Effect of valine on the activity of *bsTD*. (A) Initial velocity of threonine deamination by *bsTD* as a function of valine concentration in the presence of 10 (▲), 20 (■), or 50 mM threonine (○). (B) Initial velocity of threonine deamination by *bsTD* as a function of valine concentration in the absence of isoleucine (●) and in the presence of 0.15 (■), 0.3 (▲), or 0.9 mM (▽) isoleucine, with 20 mM threonine. The lines in both figures are the theoretical fits to eq 4, with the parameters of Table 4 for the wild-type enzyme.

and the assumption that in *bsTD* the regulatory sites must be in the interface of a regulatory dimer. In the model, we further assumed that the two regulatory domains contributed by a pair of *bsTD* protomers (Figure 2D) are related by a symmetric 2-fold axis as in the ACT domain family (*21*). This working model and the effector sites mapped in the mutational studies of *ecTD* and *atTD* (*4, 14, 20*) were used to suggest residues which might be located in or near the effector binding site in *bsTD*.

Analysis of Mutations in the Putative Effector Site. We prepared mutants modified at each of the six positions shown in Figure 6. Four of the mutants, Q347A, L352A, T367A, and Y371L, were fully characterized and analyzed using the modified MWC model (eq 4), and the results are summarized in Table 4. The remaining two, G350A and N363A, were only partially characterized (data not shown). The preliminary properties of N363A were so similar to those of the wild type that there is little basis for assuming that Asn363 interacts with either of the effectors. Although mutant G350A showed some deviation from the wild-type characteristics in its responses to isoleucine and valine (Figure 7), we did not continue its investigation as any mutation of a glycine residue in a loop would affect the chain conformation, making any conclusions ambiguous.

In mutant Y371L, homologous (see Figure 1 of the Supporting Information) to the regulatory domain variants Y449L and Y543L in *atTD* characterized by Wessel et al. (*14*), the apparent affinities for both of the allosteric effectors are very low (Figure 8). The apparent dissociation constant for isoleucine from the T state (K_T^{Ile}) was 50-fold higher than that of the wild type. The ability of valine to counter the inhibition caused by isoleucine was almost completely abolished (Figure 8B). The affinity for threonine was considerably lower than in the wild type, with a constant for dissociation from the R state (K_R^S) of 27 ± 3 mM, 4.5-fold higher than that of the wild type. The overall equilibrium between the T and R conformational states of the protein, *L*, was without change (Table 4). In mutant L352A, homologous to the *ecTD* regulatory domain variant L447F characterized by Eisenstein et al. (*17, 18*), the affinity for both allosteric effectors was lower, with K_T^{Ile} and K_R^{Val} 7- and 5-fold higher, respectively, than in the wild type. The affinity for the substrate was lowered, as it was in Y371L. The kinetic data could be fit only using the assumption that $c_V \sim 0$, i.e., that valine binds exclusively to the R state. It is fascinating to note that an activating effect of valine was observed in this mutant (and in mutant G350A), even in the absence of isoleucine (Figure 7). It seems that this mutation caused a shift in the equilibrium between the T and R conformational states of the protein toward the T state; i.e., *L* was 6.5-fold higher than that of the wild type.

Residue T367 is fully conserved in the single-regulatory domain TDs and in the first subdomains of the long variety TDs. In the homologous position in the second subdomain, it is conserved either as Thr or as Ser, the other small hydroxyl-containing polar amino acid. We thought that it might be a good candidate for interacting with the allosteric effectors, as the homologous residue S461 in the crystal structure of *ecTD* (*20*) is in the proximity of Y369 (homologous to Y371 in *bsTD*). The T367A mutation caused a decrease in the affinity of *bsTD* for both allosteric effectors (Table 4). This was the only mutant in which the substrate affinity was increased ($K_R^S = 3.6 \pm 0.4$ mM compared to 6.0 ± 0.4 mM in the wild type).

The position of Q347 is conserved as Glu in all the TDs with two ACT-like subdomains and as Gln in all the single-regulatory domain TDs (Figure 1 of the Supporting Information). This and its similarity in position and polarity to the conserved Asn residue in the ACT domain family (*21*) made this Gln a good candidate for mutagenesis. Mutant Q347A was very similar to the wild-type enzyme in most of its characteristics, except for a 1.5-fold increase in *L* and a 5-fold increase in K_T^{Ile}.

DISCUSSION

Allosteric Regulation Model for bsTD. We have shown that an allosteric model that is based on the classical MWC model could account for our results (*7*). We assume that *bsTD* is in equilibrium between two states: a tense (T) state with a relatively low affinity for threonine and a relaxed (R) state with a relatively high affinity for threonine. Upon addition of threonine or AB, the T to R equilibrium is shifted toward the R state, thus giving rise to positive cooperativity in threonine deamination or AB binding. Isoleucine is an allosteric inhibitor that binds preferentially at regulatory sites

Table 4: MWC Analysis of the Steady-State Kinetics for the Wild Type and Four Mutant Forms of *bsTD*

parameter[a]	wild type	Y371L	T367A	L352A	Q347A
L	2.61 ± 0.13	2.65 ± 0.70	2.26 ± 0.09	17 ± 4	4.05 ± 0.71
K_R^S (mM)	6.02 ± 0.36	26.9 ± 2.8	3.64 ± 0.41	26 ± 2	6.6 ± 0.2
c_S	0.149 ± 0.012	0.307 ± 0.013	0.239 ± 0.020	0.24 ± 0.02	0.21 ± 0.01
K_T^S (mM)[b]	40.4 ± 4.1	87.6 ± 9.9	15.2 ± 2.1	116 ± 13	31.4 ± 1.8
K_R^{Ile} (mM)	0.379 ± 0.028	14.8 ± 1.3	2.48 ± 0.29	1.14 ± 0.18	1.74 ± 0.10
c_I	3.50 ± 0.19	2.56 ± 0.12	3.60 ± 0.27	1.49 ± 0.03	3.32 ± 0.14
K_T^{Ile} (mM)[b]	0.11 ± 0.01	5.8 ± 0.6	0.69 ± 0.10	0.77 ± 0.12	0.52 ± 0.04
K_R^{Val} (mM)	2.30 ± 0.33	9.8 ± 1.7[c]	5.70 ± 0.77	11.6 ± 4.3[d]	2.4 ± 0.3
c_V	1.00 ± 0.07	1.19 ± 0.02 [c]	0.98 ± 0.05	0 ± 0.3[d]	0.73 ± 0.05
K_T^{Val} (mM)[b]	2.3 ± 0.4	11.6 ± 2.0[c]	5.8 ± 0.8	>3[d]	3.3 ± 0.5
$K_{R(act)}^{Val}$ (mM)	223 ± 23	[223][c]	260 ± 32	[223][d]	293 ± 45
c_{Vin}	1.52 ± 0.70	[1.52][c]	0.2 ± 0.5	[1.52][d]	1.0 ± 0.9 ($P \sim 0.28$)

[a] Parameters of eqs 2 and 4 as defined above. [b] The dissociation constants of the effectors from the regulatory sites and of threonine from the substrate sites in the T state (K_T in each case) were calculated from best fit values of the same dissociation constants in the R state (K_R) and the ratio of dissociation constants of the ligand from the R and T conformations (c_s): $K_T = cK_R$. Errors were calculated from errors in the individual parameters. [c] For mutant Y371L, the apparent activation effect of valine is so weak that it is difficult to separate from its competition with substrate (Figure 8B). We fit the data using the arbitrary assumption that the affinity of valine for the substrate site is similar to that of the wild type, and these parameters are given in brackets. [d] For mutant L352A, c_V and c_{Vin} tend to 0 when the data are fit to eq 4. We fit the data using the arbitrary assumption that the affinity of valine for the substrate site is similar to that of the wild type, and these parameters are given in brackets.

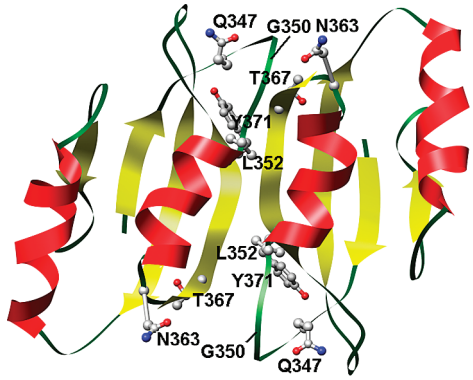

FIGURE 6: Working model for the regulatory domain dimer of *bsTD* (as in Figure 2D) with the side chains mutated in this study shown in ball-and-stick format.

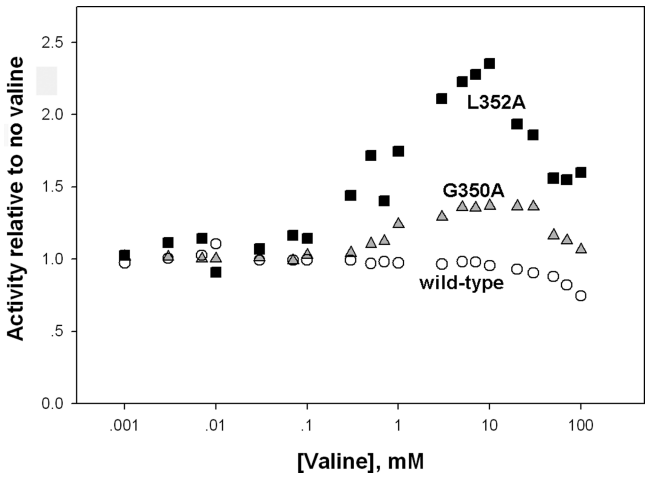

FIGURE 7: Effect of valine on the activity of the wild type and two mutants of *bsTD* under comparable conditions, normalized to activity in the absence of valine. The threonine deaminase activities of the purified enzymes were measured at 45 mM threonine [wild type (○)] or 50 mM threonine [G350A (▲) and L352A (■)], in the presence of various concentrations of valine.

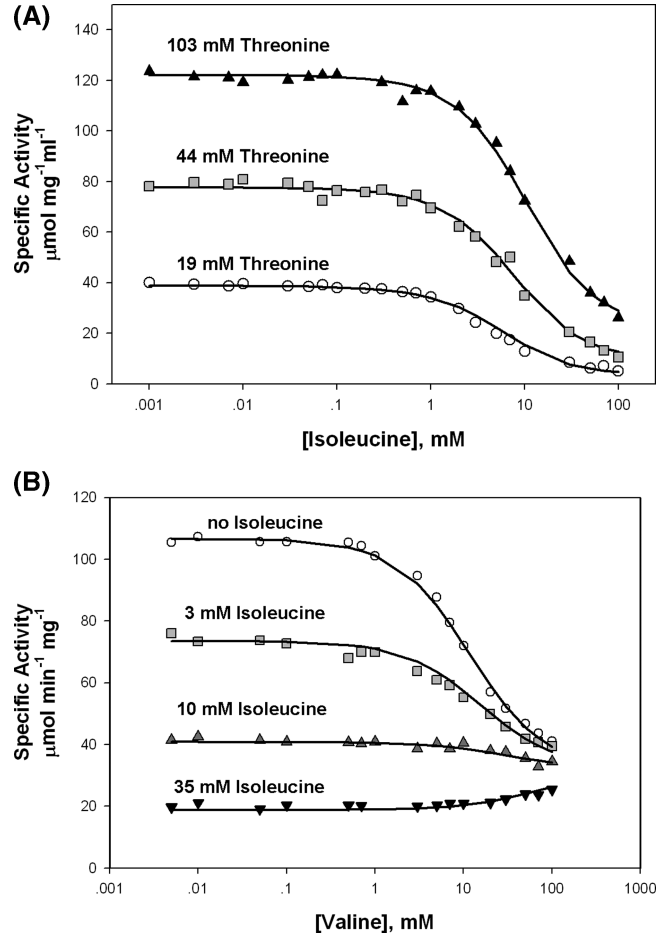

FIGURE 8: Effector responses of *bsTD* mutant Y371L. (A) Initial velocity of threonine deamination by *bsTD* Y371L as a function of isoleucine concentration in the presence of 19 (○), 44 (■), or 103 mM threonine (▲). (B) Initial velocity of deamination of threonine (44 mM) by *bsTD* Y371L as a function of valine concentration in the absence of isoleucine (○) and in the presence of 3 (■), 10 (▲), or 35 mM isoleucine (▼).

in the T state, thus increasing positive cooperativity in threonine deamination or AB binding. Because isoleucine inhibition of *bsTD* activity levels off at saturating isoleucine concentrations and does not decrease to zero (Table 2 and Figure 4A), we conclude that isoleucine binds nonexclusively, to both the T and R states [$c_I = 3.50$ (Table 3)] (*32*).

The value obtained for the allosteric constant *L* is quite low and the value obtained for *c*, the ratio of threonine affinities for the T and R conformations, high relative to the values determined for the *ecTD* enzyme by Eisenstein and colleagues (*17*). In the framework of the MWC model (*7*), this implies a relatively low magnitude of cooperativity in substrate binding by *bsTD*, in agreement with the low values of the Hill coefficient obtained for this system (Figure 3).

Complex activation and inhibition effects of valine on *bsTD* activity are observed (Figure 5B). Biphasic effects of ligands which compete with substrate, and thus favor the R state, have been demonstrated in a few other allosteric enzymes (*33, 34*). It is very unlikely that such an effect occurs in the case of *bsTD*, in light of the behavior of the mutants described here. The properties of the variant enzymes mutated in the putative effector binding domain support the conclusion that the activating effect of valine is due to its binding to the effector sites, while its inhibitory effect is caused by its binding to the catalytic sites in competition with threonine. In terms of the proposed modified MWC model of eq 4, at low concentrations valine binds to regulatory sites of *bsTD* with little preference for either of the allosteric states (Table 4). Valine leads to the apparent activation of the enzyme only under conditions where the allosteric equilibrium would otherwise be shifted more toward the T state, either by the presence of isoleucine or by a mutation, e.g., L352A (Table 4). At concentrations ~100-fold higher, valine also binds to a site at which it inhibits. This inhibition is countered by higher substrate concentrations (Figure 5A). Analysis of our data with the model assuming that this second site is the catalytic site gives a satisfactory fit. We therefore conclude that competition at the substrate site is in fact the mechanism for valine inhibition of *bsTD*. Valine is isosteric with threonine, and it is reasonable to expect that it can bind in the active site, albeit with a much lower affinity than the substrate. The binding of valine to the regulatory site in the wild-type enzyme, with an affinity some 6-fold lower than that of isoleucine and little preference for one allosteric conformation or the other, can be rationalized by its smaller size, with one fewer methyl group than isoleucine.

This description of the results in the framework of the MWC model was cast into an equation that takes into account all the features of the model described above (eq 4). Global fitting to eq 4 performed simultaneously on all steady-state catalysis data for the wild-type enzyme in the presence and absence of isoleucine yielded very good fits with an overall correlation coefficient of 0.99 for the steady-state catalysis (Figures 3 and 4). The parameters for interaction with valine were found subsequently by fitting the steady-state catalysis data in the presence of valine assuming the other parameters were known (Figure 5). The equation can also fit substrate analogue (AB) binding data and accommodate effects of isoleucine on AB binding data (Figure 4B). The catalysis data for each of the fully characterized mutants can also be rationalized using the same model (Table 4). Other MWC-based models, including the one suggested by Eisenstein and colleagues for the *ecTD* enzyme (*17*), failed to fit the data.

It should be emphasized that the values obtained independently for threonine deamination and for substrate analogue binding are similar in magnitude. In particular, the value of the allosteric constant *L* is similar in both AB binding and threonine deamination data (Table 3). Since *L* reports on the conformational equilibrium of *bsTD* in the absence of any ligands, the fact that similar values were obtained in both binding and catalysis data, combined with the similar Hill coefficient values obtained for *bsTD* in both analyses, suggests that cooperativity in *bsTD* is a *K* system rather than a *V* system, i.e., that cooperativity in *bsTD* function arises predominantly from ligand binding effects and not from the different catalytic powers of the two conformers (*7*).

The allosteric model for *bsTD* proposed here is different from the modified MWC model suggested for the archetypal TD from *E. coli* by Eisenstein and colleagues (*17*) and supported by their experiments on *ecTD*. In the *ecTD* model, the substrate threonine binds exclusively to the R state, whereas in *bsTD*, it binds to both T and R states (models that consider exclusive threonine binding to *bsTD* failed to fit the data). Second, the allosteric inhibitor isoleucine was demonstrated to bind exclusively to the T state of the *ecTD* enzyme but nonexclusively to *bsTD*. Third, in the *ecTD* enzyme, threonine competes with valine and isoleucine for binding at their regulatory sites in the R and T states, respectively, whereas in the *bsTD* enzyme, no support for such a finding is obtained. Lastly, in the *ecTD* enzyme, valine binds only to regulatory sites in the R state, whereas for *bsTD*, valine competes with threonine for binding at the catalytic sites as well as competing with isoleucine for the regulatory sites. Although, in general, both *ecTD* and *bsTD* are inhibited by isoleucine and activated by valine, the detailed allosteric regulation pattern and mechanism of these enzymes are different. It should be noted that the values for *L* (1525) and for *c* (0) obtained for *ecTD* (*17*) are much higher and lower, respectively, than the ones obtained for *bsTD*, reflecting the higher cooperativity in TD function for *ecTD*. The difference in cooperativity is seen in the Hill coefficient values, independent of models.

Can we rationalize the differences in the regulation patterns of *ecTD* and *bsTD* on the basis of available sequence and structural data (*21*) (Figure 2B,D)? Eisenstein concluded from a combination of structural and functional data on *ecTD* that only one molecule of either valine or isoleucine can bind at the interface between the two subdomains of the regulatory domain (*18*). However, a sequence and structural comparison of *ecTD* to the regulatory domain of 3-PGDH (*17*), the prototypic ACT domain (*21*), suggests it should be capable of binding two effector molecules in two binding sites related by a pseudosymmetry axis. Eisenstein suggested that this implies a negative cooperativity between the potential effector binding sites of the regulatory units in the case of *ecTD*. Negative cooperativity between the isoleucine effector binding sites is absent, however, in the case of *atTD*, as for this enzyme eight isoleucine molecules were shown to bind one TD tetramer (*14*). Since *bsTD* lacks one of the two subdomains that comprise the regulatory unit [Figure 2 and Figure 1 of the Supporting Information (*4, 20, 21*)], and since it still binds its allosteric effectors, it is reasonable to speculate that *bsTD* regulatory units are composed of two domains contributed from two different adjacent subunits. If this is correct, then *bsTD* contains two regulatory units organized around the four catalytic domains, with two identical symmetry-related sites in each regulatory unit. We suggest that two molecules of the allosteric effector valine

or isoleucine are bound at each regulatory unit, as in the case of the *atTD* enzyme (*14*). This suggestion is supported by the properties of mutant enzymes: mutations at four different positions each affect the affinities for isoleucine and valine. Threonine 367 is far from the three other positions examined here, based on any reasonable model, and the only way to rationalize this is by assuming the dimerization of the regulatory domains in *bsTD* with 2-fold symmetry (Figure 6). Efforts to determine the structure of the *bsTD* protein are underway in our laboratories to validate the quaternary organization of the proposed model.

Valine Inhibition of bsTD. The obvious differences between the regulatory domains in the *bsTD* and *ecTD* enzymes can explain several of the differences in the allosteric regulation schemes of these enzymes by valine and isoleucine. However, this does not explain why competition of valine with threonine for binding to the catalytic sites is evident in the *bsTD* enzyme, while such competition has not been reported for *ecTD* or *atTD*. Examination of the active site residues involved in binding of the PLP cofactor (*20*) (Figure 1 of the Supporting Information) reveals that most of the residues, including (*E. coli* sequence numbering) K62, N89, S315, and the tetraglycine loop (residues 188−191), are conserved. There are, however, a few sequence differences at nonconserved positions in the region of possible contacts with threonine (or valine) bound as the internal imine of PLP (*20*) in the *E. coli* (see Protein Data Bank entry 1TDJ) and *B. subtilis* TD (e.g., P155 in *ecTD* is H154 in *bsTD*). Such sequence differences might lead to differences between these enzymes in their affinities for valine as a competitive inhibitor. On the other hand, it is not clear that competition of valine with threonine would not be masked by the activating effects of valine at the regulatory sites of the long sequence varieties of TD. Furthermore, in searching for valine activation of *bsTD*, we have examined high valine concentrations which may not have been tested in studies of *ecTD* or *atTD*.

The physiological advantage of the complex regulation patterns of threonine deaminases has been understood by considering the cross talk between the competing valine and isoleucine biosynthetic pathways (Figure 1) and from the observation that 2-ketobutyrate accumulation exerts a toxic effect on *Salmonella typhimurium* (*35*) and on *B. subtilis* cells (*36*). TD converts threonine to 2-ketobutyrate and is regulated by valine and isoleucine, the end products of two competing pathways. Acetohydroxyacid synthase (AHAS) catalyzes the condensation of pyruvate with either 2-ketobutyrate or another pyruvate molecule, thus controlling the relative fluxes along the isoleucine and valine/leucine pathways. At low and moderate concentrations, valine activation of TD pushes the flux toward isoleucine synthesis and thus balances the synthesis of isoleucine with that of valine and leucine (Figure 1). High valine concentrations cause partial inhibition of AHAS from enterobacterial (*5*) and *Bacillus* species (*37*; E. Zalyapin, unpublished data) and may thus bring about accumulation of toxic levels of 2-ketobutyrate. However, in contrast to valine inhibition of AHASs, the concentrations of valine required to have a significant inhibitory effect on *bsTD* ($\geq$10 mM) are very unlikely to prevail in vivo. The apparent affinity of the active site of *bsTD* for valine in the R state is some 40-fold lower than its affinity for threonine, so that it seems unlikely that it would be a physiologically effective response. It seems more likely to be a result of the physical−chemical limits of the specificity of this protein.

Evolution of Structural Differences between "Short" and "Long" TDs. The response of *bsTD* to valine as a positive effector is quite limited compared to that observed for, for example, *ecTD.* Because of the physical−chemical limits of the effect of a single methyl group on ligand−protein interactions, one and the same effector site can not have large, opposed conformational effects on the binding of valine or isoleucine. One generally recognized mechanism for protein evolution is the repetition of a fragment of a sequence, and it is easy to conceive of such a repetition of an ACT-like sequence leading to a mutated TD with a long regulatory domain. This long repeat of an ACT-like sequence can fold to create a regulatory domain with intrasubunit as opposed to intersubunit effector binding sites (e.g., ref *20*). Such a domain would no longer necessarily have 2-fold symmetry, and its sequence would be free to evolve to create a pair of sites with different effector specificities and possible mutual allosteric effects. As bacterial species evolved to exploit the complex and changing media of commensual life within the digestive tracts of multicellular organisms (e.g., the enterobacteria), they would have been able to benefit from more sophisticated control of biosynthetic pathways. The enterobacteria have multiple AHAS isozymes and "long version" TDs in their pathways to the branched chain amino acids, which allow them to grow in varied media. This hypothetical scheme for the development of the two types of biosynthetic TDs might be tested by determination of the structure of *bsTD*.

ACKNOWLEDGMENT

We are grateful to Prof. C. R. Harwood at the University of Newcastle (Newcastle, Australia) for kindly providing us with the *B. subtilis* 168 strain. We thank Dr. I. Fishov and A. Aronovich for their help with fluorescence studies, Karsten Dierks and Sharon Vanunu for assistance with dynamic light scattering analysis, and M. Einav for technical assistance and helpful discussions during this study. We thank Dr. N. Zilberberg for critical reading of the manuscript.

SUPPORTING INFORMATION AVAILABLE

Sequence alignment of TDs from different sources, along with the secondary structure of *ecTD* (Figure 1). This material is available free of charge via the Internet at http://pubs.acs.org.

REFERENCES

1. Pardee, A. B., and Reddy, G. P. (2003) Beginnings of feedback inhibition, allostery, and multi-protein complexes. *Gene 321*, 17–23.
2. Changeux, J. P. (1993) Allosteric proteins: From regulatory enzymes to receptors-personal recollections. *BioEssays 15*, 625–634.
3. Umbarger, H. E. (1992) The origin of a useful concept—feedback inhibition. *Protein Sci. 1*, 1392–1395.
4. Gallagher, D. T., Chinchilla, D., Lau, H., and Eisenstein, E. (2004) Local and global control mechanisms in allosteric threonine deaminase. *Methods Enzymol. 380*, 85–106.
5. Umbarger, H. E. (1990) The study of branched chain amino acid biosynthesis: Its roots and its fruits, in *Biosynthesis of Branched Chain Amino Acids* (Barak, Z., Chipman, D. M., and Schloss, J. V., Eds.) pp 1−24, VCH, Weinheim, Germany.

6. Changeux, J. P. (1961) The feedback control mechanism of biosynthetic L-threonine deaminase by L-isoleucine. *Cold Spring Harbor Symp. Quant. Biol. 26*, 313–330.
7. Monod, J., Wyman, J., and Changeux, J.-P. (1965) On the nature of allosteric transitions: A plausible model. *J. Mol. Biol. 12*, 88–118.
8. Betz, J. L., Hereford, L. M., and Magee, P. T. (1971) Threonine deaminases from *Saccharomyces cerevisiae* mutationally altered in regulatory properties. *Biochemistry 10*, 1818–1824.
9. Maeba, P., and Sanwal, B. D. (1966) The allosteric threonine deaminase of *Salmonella*. Kinetic model for the native enzyme. *Biochemistry 5*, 525–536.
10. Zarlengo, M. H., Robinson, G. W., and Burns, R. O. (1968) Threonine deaminase from *Salmonella typhimurium*. II. The subunit structure. *J. Biol. Chem. 243*, 186–191.
11. Calhoun, D. H., Rimerman, R. A., and Hatfield, G. W. (1973) Threonine deaminase from *Escherichia coli*. I. Purification and properties. *J. Biol. Chem. 248*, 3511–3516.
12. Decedue, C. J., Hofler, J. G., and Burns, R. O. (1975) Threonine deaminase from *Salmonella typhimurium*. Relationship between regulatory sites. *J. Biol. Chem. 250*, 1563–1570.
13. Eisenstein, E. (1991) Cloning, expression, purification, and characterization of biosynthetic threonine deaminase from *Escherichia coli*. *J. Biol. Chem. 266*, 5801–5807.
14. Wessel, P. M., Graciet, E., Douce, R., and Dumas, R. (2000) Evidence for two distinct effector binding sites in threonine deaminase by site-directed mutagenesis, kinetic and binding experiments. *Biochemistry 39*, 15136–15143.
15. Hatfield, G. W., and Umbarger, H. E. (1970) Threonine deaminase from *Bacillus subtilis*. II. The steady state kinetic properties. *J. Biol. Chem. 245*, 1742–1747.
16. Eisenstein, E. (1994) Energetics of cooperative ligand binding to the active sites of threonine deaminase. *J. Biol. Chem. 269*, 29416–29422.
17. Eisenstein, E., Yu, H. D., Fisher, K. E., Iacuzio, D. A., Ducote, K. R., and Schwarz, F. P. (1995) An expanded two-state model accounts for homotropic cooperativity in biosynthetic threonine deaminase from *Escherichia coli*. *Biochemistry 34*, 9403–9412.
18. Eisenstein, E., Yu, H. D., and Schwarz, F. P. (1994) Cooperative binding of the feedback modifiers isoleucine and valine to threonine deaminase. *J. Biol. Chem. 269*, 29423–29429.
19. Chinchilla, D., Schwarz, F. P., and Eisenstein, E. (1998) Amino acid substitutions in the C-terminal regulatory domain disrupt allosteric effector binding to biosynthetic threonine deaminase from *Escherichia coli*. *J. Biol. Chem. 273*, 23219–23224.
20. Gallagher, D. T., Gilliland, G. L., Xiao, G., Zondlo, J., Fisher Kathryn, E., Chinchilla, D., and Eisenstein, E. (1998) Structure and control of pyridoxal phosphate dependent allosteric threonine deaminase. *Structure 6*, 465–475.
21. Chipman, D. M., and Shaanan, B. (2001) The ACT domain family. *Curr. Opin. Struct. Biol. 11*, 694–700.
22. Schuller, D. J., Grant, G. A., and Banaszak, L. J. (1995) The allosteric ligand site in the V_{max}-type cooperative enzyme phosphoglycerate dehydrogenase. *Nat. Struct. Biol. 2*, 69–76.
23. Eisenstein, E. (1995) Allosteric regulation of biosynthetic threonine deaminase from *Escherichia coli*: Effects of isoleucine and valine on active-site ligand binding and catalysis. *Arch. Biochem. Biophys. 316*, 311–318.
24. Garcia, E. L., and Mourad, G. S. (2004) A site-directed mutagenesis interrogation of the carboxy-terminal end of *Arabidopsis thaliana* threonine dehydratase/deaminase reveals a synergistic interaction between two effector-binding sites and contributes to the development of a novel selectable marker. *Plant Mol. Biol. 55*, 121–134.
25. Engel, S., Vyazmensky, M., Vinogradov, M., Berkovich, D., Bar-Ilan, A., Qimron, U., Rosiansky, Y., Barak, Z., and Chipman, D. M. (2004) Role of a conserved arginine in the mechanism of acetohydroxyacid synthase: Catalysis of condensation with a specific ketoacid substrate. *J. Biol. Chem. 279*, 24803–24812.
26. Ho, S. N., Hunt, H. D., Horton, R. M., Pullen, J. K., and Pease, L. R. (1989) Site-directed mutagenesis by overlap extension using the polymerase chain reaction. *Gene 77*, 51–59.
27. Hatfield, G. W., and Umbarger, H. E. (1970) Threonine deaminase from *Bacillus subtilis*. I. Purification of the enzyme. *J. Biol. Chem. 245*, 1736–1741.
28. Penefsky, H. S. (1977) Reversible binding of Pi by beef heart mitochondrial adenosine triphosphatase. *J. Biol. Chem. 252*, 2891–2899.
29. Hill, A. V. (1910) The possible effects of the aggregation of the molecules of heamoglobin on its oxygen dissociation curve. *J. Physiol. (Oxford, U.K.) 40*, IV–VII.
30. Levitzki, A. (1978) *Quantitative aspects of allosteric mechanisms*, pp 38−44, Springer-Verlag, Berlin.
31. Mockel, B., Eggeling, L., and Sahm, H. (1994) Threonine dehydratases of *Corynebacterium glutamicum* with altered allosteric control: Their generation and biochemical and structural analysis. *Mol. Microbiol. 13*, 833–842.
32. Rubin, M. M., and Changeux, J. P. (1966) On the nature of allosteric transitions: Implications of non-exclusive ligand binding. *J. Mol. Biol. 21*, 265–274.
33. Gerhart, J. C., and Pardee, A. B. (1963) Effect of the feedback inhibitor, CTP, on subunit interactions of aspartic transcarbamylase. *Cold Spring Harbor Symp. Quant. Biol. 28*, 491–496.
34. Horovitz, A., Fridmann, Y., Kafri, G., and Yifrach, O. (2001) Review: Allostery in chaperonins. *J. Struct. Biol. 135*, 104–114.
35. LaRossa, R. A., VanDyk, T. K., and Smulski, D. R. (1987) Toxic accumulation of α-ketobutyrate caused by inhibition of the branched-chain amino acid biosynthetic enzyme acetolactate synthase in *Salmonella typhimurium*. *J. Bacteriol. 169*, 1372–1378.
36. Lamb, D. H., and Bott, K. F. (1979) Inhibition of *Bacillus subtilis* growth and sporulation by threonine. *J. Bacteriol. 137*, 213–220.
37. Porat, I., Vinogradov, M., Vyazmensky, M., Lu, C.-D., Chipman, D. M., Abdelal, A. T., and Barak, Z. (2004) Cloning and Characterization of Acetohydroxyacid Synthase from *Bacillus stearothermophilus*. *J. Bacteriol. 186*, 570–574.
38. Bennett-Lovsey, R. M., Herbert, A. D., Sternberg, M. J., and Kelley, L. A. (2008) Exploring the extremes of sequence/structure space with ensemble fold recognition in the program Phyre. *Proteins 70*, 611–625.

BI800901N